Talanta 83 (2010) 332–336

Contents lists available at ScienceDirect

Talanta

journal homepage: www.elsevier.com/locate/talanta

Simultaneous determination of Cd(II) and Pb(II) by differential pulse anodic stripping voltammetry based on graphite nanofibers–Nafion composite modified bismuth film electrode

Dongyue Li[b], Jianbo Jia[a,*], Jianguo Wang[b,*]

[a] State Key Laboratory of Electroanalytical Chemistry, Changchun Institute of Applied Chemistry, Chinese Academy of Sciences, 5625 Renmin Street, Changchun, Jilin 130022, PR China
[b] College of Chemistry, Liaoning University, Shenyang, Liaoning 110036, PR China

ARTICLE INFO

Article history:
Received 30 May 2010
Received in revised form
10 September 2010
Accepted 18 September 2010
Available online 25 September 2010

Keywords:
Graphite nanofibers
Nafion
Bismuth film
Cadmium
Lead
Stripping voltammetry

ABSTRACT

A bismuth-film modified graphite nanofibers–Nafion glassy carbon electrode (BiF/GNFs–NA/GCE) was constructed for the simultaneous determination of trace Cd(II) and Pb(II). The electrochemical properties and applications of the modified electrode were studied. Operational parameters such as deposition potential, deposition time, and bismuth ion concentration were optimized for the purpose of determination of trace metal ions in 0.10 M acetate buffer solution (pH 4.5). Under optimal conditions, based on three times the standard deviation of the baseline, the limits of detection were 0.09 $\mu g\,L^{-1}$ for Cd(II) and 0.02 $\mu g\,L^{-1}$ for Pb(II) with a 10 min preconcentration. In addition, the BiF/GNFs–NA/GCE displayed good reproducibility and selectivity, making it suitable for the simultaneous determination of Cd(II) and Pb(II) in real sample such as river water and human blood samples.

1. Introduction

Anodic stripping voltammetry has been established as a powerful tool for the determination of trace metal ions, owning to an effective preconcentration step with advanced electrochemical measurements of the accumulated analytes [1–4]. In previous studies, mercury electrodes were used for achieving high sensitivity and reproducibility [5]. However, the environmental regulations and health considerations restrict its continuous application due to the high toxicity of mercury. Recently, bismuth film electrode (BiFE) has drawn considerable interests in the field of the stripping technique because of its remarkable low toxicity and the ability to form alloy with many metals as well as its partial insensitivity to dissolved oxygen, wide potential window, which has proved to be equal to or even superior to that of mercury film electrode [3,4,6–10]. Though various chemically modified electrodes have been exploited for anodic stripping voltammetric determination of trace metals, such as functionalized mesoporous silica electrode [11], carbon nanotubes (CNTs) modified electrode [12,13], ordered mesoporous carbon (OMC) [14], nanocrystalline diamond thin-film electrode [15] and graphene [16,17] modified electrodes, we still need new materials to improving the detection sensitivity and reproducibility in analysis of trace metals.

Graphite nanofibers (GNFs) have cylindrical nanostructure with the anisotropic alignment of graphene layers such as platelet, herringbone and tubular axis [18]. As a promising kind of carbon materials, GNFs have drawn increasing attention due to their mechanical stability, high electrical conductivity, large surface active groups, and easy mass production. In addition, activation of GNFs with nitric acid can produce a range of oxygen-containing groups without degradation of the structural integrity of their backbone, leading to better dispersion and wettability [19,20]. The GNFs possess less order and more edge sites on the outer wall than those of CNTs [21], which facilitate the electron transfer of electroactive analytes. On the other hand, in order to alleviate interferences and improve the mechanical stability, Nafion (NA) was widely used as coating ionomer. Previous results have shown that NA membrane can enrich metal cations, improve voltammetric signal-to-noise ratios, and increase the electrode's resistance against fouling by surface-active compounds effectively [22,23].

In this work, a sensitive platform for the detection Cd(II) and Pb(II) was presented based on the GNFs–NA modified glassy carbon electrode (GNFs–NA/GCE) which remarkably enhances the stripping performances. The surface morphology of the electrode was characterized by scanning electron microscopy (SEM). The

---

* Corresponding authors. Tel.: +86 431 85262378; fax: +86 431 85685653.
E-mail addresses: jbjia@ciac.jl.cn (J. Jia), jgwang@lnu.edu.cn (J. Wang).

0039-9140/$ – see front matter © 2010 Elsevier B.V. All rights reserved.
doi:10.1016/j.talanta.2010.09.024

as-prepared electrode was applied to the determination of trace metals in river water and blood samples, and the results were compared with those of inductively coupled plasma mass spectrometry (ICP-MS).

2. Experiment

2.1. Apparatus

Cyclic voltammetry (CV) and differential pulse anodic stripping voltammetry (DPASV) were performed in a conventional three-electrode cell with a CHI 832B electrochemical workstation (CH Instruments, Shanghai, China). The modified GCE (3 mm diameter) was used as the working electrode. An Ag/AgCl (saturated KCl) electrode and a platinum foil were used as the reference electrode and auxiliary electrode, respectively. SEM images were obtained from an XL 30 ESEM FEG SEM (Philips, Netherlands) with an accelerating voltage of 20 kV. For the ICP-MS measurements of Cd(II) and Pb(II), an X SeriesII ICP-MS (Thermo Scientific, USA) was used. All the electrochemical experiments were carried out in a one-compartment electrochemical cell at room temperature (20 ± 1 °C).

2.2. Reagents and solutions

GNFs (>95%, O.D. × I.D. × L 80–200 nm × 0.5–10 nm × 0.5–20 μm) and NA (5 wt% in a mixture of lower aliphatic alcohols and lower) were purchased from Aldrich. Single-walled carbon nanotubes (SWNTs) were obtained from Shenzhen Nanotech Port Co., Ltd. (China). Hexaammineruthenium(III) chloride (98%) was obtained from J&K Chemical Ltd. A 0.10 M acetate buffer (pH = 4.5) prepared by mixing appropriate amounts of CH_3COOH and CH_3COONa was served as the supporting electrolyte. All the other chemicals were analytical grade, or better, and used as received. Unless otherwise stated, all the solutions were prepared with pure water from Water Purifier (Sichuan Water Purifier Co., Ltd., China).

2.3. Treatment of graphite nanofibers

Twenty milligrams of GNFs was dispersed in 30 mL of 30% HNO_3, and the resultant mixture was then refluxed for 24 h at 140 °C [12]. The resulting suspension was centrifuged and the precipitate was washed with 0.10 M NaOH to neutralize to pH 7.0. The washed GNFs were collected and dried at 100 °C overnight. This treatment made carboxylation of GNFs at the terminus. The SWNTs were treated as the method as GNFs.

2.4. Fabrication of GNFs–NA film coated GCE

Ultrasonic for 30 min was used to disperse the carboxylic GNFs into N,N-dimethylformamide until a homogeneous suspension resulted. Then, a 50 μL of 2 mg mL^{-1} GNFs suspension was mixed with 450 μL 0.5 wt% NA ethanol solution by ultrasonication for 30 min. Between each modification, the GCE was polished carefully with smaller grades of alumina slurries (1.0, 0.3, and 0.05 μm) respectively, followed by sonicated in 1:1 nitric acid, acetone and pure water after each stage of polishing successively and dried under nitrogen. Then, an aliquot of 3 μL of the mixture was coated on the GCE, and then the solvent was evaporated under an infrared lamp to obtain the GNFs-NA/GCE. For comparison, SWNTs-NA composite film electrode (SWNTs-NA/GCE) was prepared in the same manner.

2.5. Procedure for DPASV analysis

Bismuth was in situ deposited onto the modified electrode, from non-deaerated 0.10 M acetate buffer (pH 4.5) in the presence of 400 μg L^{-1} Bi(III) with model target metals, if not stated otherwise. The preconcentration step was carried out at −1.2 V for 120 s while stirring the solution. After a 10 s equilibration period, the voltammogram was recorded by applying a positive-going potential scan from −1.2 to 0.3 V (with a step increment of 5 mV, amplitude of 80 mV, pulse period of 0.2 s, and pulse width of 5 ms). Prior to the next cycle, a preconditioning step (120 s at 0.3 V, with solution stirring) was used to remove the target metals and bismuth film. River water was collected from Yongchun River in Changchun, and was filtered through a 0.45 μm membrane (Millipore). Human blood samples were obtained from the local hospital and digested with nitric acid–perchloric acid in 70 °C water bath pan into pre-digested till a dark brown liquid appears. Then it was transferred to electric panel bath and steamed until almost dry up [24]. The samples were diluted appropriately before determination.

3. Results and discussion

3.1. SEM images of GNFs–Nafion film

SEM can take useful insights into the growth patterns of the bismuth film. The SEM image of the bismuth-coated GCE indicates a highly porous, three-dimensional fibril-like network [6]. The SEM of the GNFs film displayed a chemically lean, three-dimensional homogeneous incompact structure [25]. Fig. 1 shows SEMs of GNFs–NA/GCE before (A) and after (B) the deposition of bismuth film, respectively. As shown in Fig. 1(A), the GNFs dispersed in NA were observed with diameters ranging from 120 to 150 nm, and the surface of GNFs was smooth. From Fig. 1(B), the bismuth deposits, which can greatly enhance the electrochemically active surface area of the modified electrode, can be seen as nanoparticles on the GNFs.

3.2. Electrochemical characterization of the GNFs–NA/GCE

Two redox systems exhibiting different electrode kinetics were used to study the electrochemical properties of GNFs–NA/GCE. Fig. 2 shows the voltammograms of various redox species at the GNFs–NA/GCEs. $Fe(CN)_6{}^{4-/3-}$ proceeds through a inner-sphere electron transfer pathway while $Ru(NH_3)_6{}^{2+/3+}$ proceeds an outer sphere one [26]. Fig. 2(A) represents steady-state CVs for the bare GCE, NA/GCE and GNFs–NA/GCE in a 2.5 mM $K_3Fe(CN)_6$ solution containing 1.0 M KCl. A well-shaped CV with a peak-to-peak separation was observed at the bare GCE (solid line). When modified with NA (dashed line), the anodic and cathodic peaks almost disappeared, which indicating that the negative charged skeleton of NA acted as the blocking layer for electron and mass transfer that hinders the diffusion of $Fe(CN)_6{}^{4-/3-}$ toward the electrode surface [27]. However, the redox currents increased remarkably at the GNFs-NA/GCE (dotted line) than those of at the NA/GCE, indicating that the introduction of the graphite nanofibers could accelerate the electron transfer rate. Similar phenomena can be seen when the redox probe was changed as 2.5 mM $Ru(NH_3)_6{}^{3+}$, as shown in Fig. 2(B). The modified GCEs exhibited higher peak currents in $Ru(NH_3)_6{}^{3+}$ than those of in the same concentration of $Fe(CN)_6{}^{3-}$, which can be attributed to the negative charged NA can enrich cations while repulse anions.

The DPASV analytical characteristics of different film modified GCE, BiF/NA/GCE (dotted line), BiF/SWNTs–NA/GCE (dashed line), and BiF/GNFs–NA/GCE (solid line), by in situ plating bismuth film for trace metal determination are shown in Fig. 3. The stripping voltammograms were checked in a solution containing 20 μg L^{-1} each of Cd(II), Pb(II), and 400 μg L^{-1} Bi(III) in 0.10 M acetate buffer (pH 4.5) without deaeration. The results exhibited that the BiF/GNFs–NA/GCE takes 71% and 108% peak height

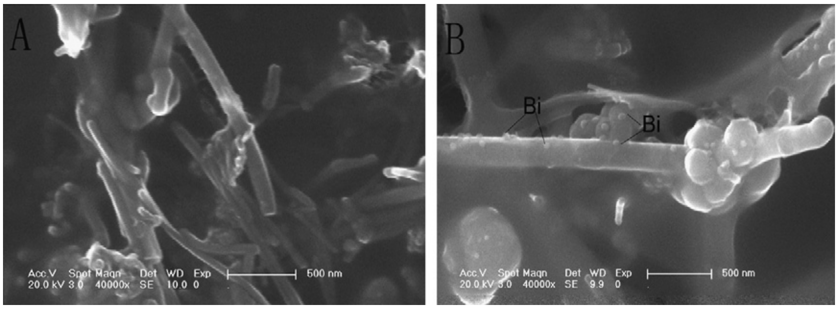

Fig. 1. SEM images of GNFs–NA/GCE (A) and BiF/GNFs–NA/GCE (B) surfaces. Deposition of bismuth film was carried out for 300 s at −1.2 V vs. Ag/AgCl with stirring, from solutions of 1000 μg L^{-1} Bi(III), 0.10 M acetate buffer (pH 4.5) as supporting electrolyte.

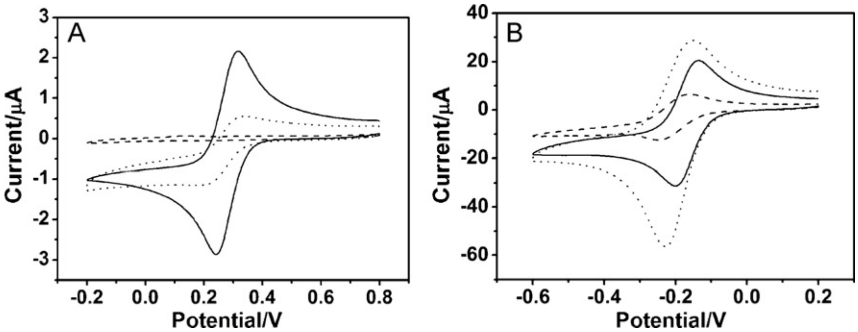

Fig. 2. CVs for bare GCE (solid line), NA/GCE (dashed line), and GNFs–NA/GCE (dotted line) in 2.5 mM $K_3Fe(CN)_6$ (A) and 2.5 mM $Ru(NH_3)_6{}^{3+}$ (B) in 1.0 M KCl, scan rate is 50 mV s^{-1}.

enhancement for Cd(II) and Pb(II) than those of BiF/NA/GCE, respectively. While under the same conditions, the BiF/SWNTs–NA/GCE improves 44% and 11% peak height enhancement for Cd(II) and Pb(II), respectively. This can be attributed to two aspects: First, GNF has high electrical conductivity, and it possesses less order and more edge sites on the outer wall which facilitate the electron transfer of electroactive analytes [19,21]. Second, the activation of GNFs with nitric acid can produce a range of oxygen-containing groups leading to better dispersion. The mixture of GNFs–NA can improve electrical conductivity so the detection sensitivities of Cd(II) and Pb(II) were enhanced.

3.3. *Effect of the experimental variables*

The voltammetric response of Cd(II) and Pb(II) was closely related to the thickness of GNFs–NA film, which was determined by the volume of GNFs–NA suspension added onto GCE surface. The relationship between the volume of GNFs–NA suspension and the stripping peak currents of Cd(II) and Pb(II) was examined, as shown in Fig. 4(A). When 3 μL of mixed polyelectrolyte was recast on the GCE, the sensitivity for Cd(II) and Pb(II) is high. However, when the amount of the coating increased from 3 to 7 μL, the peak currents were decreased, indicating that the electron transfer were blocked by thick coating on the electrode surface. According to the results, 3 μL was selected for the mixed GNFs–NA coating.

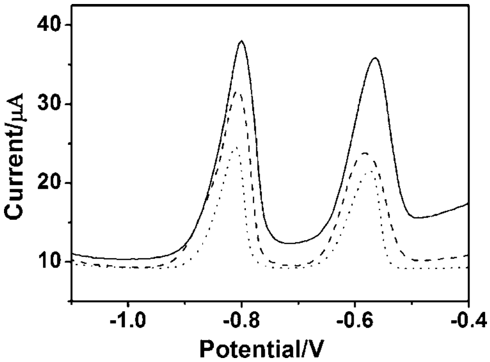

Fig. 3. DPASVs for 20 μg L^{-1} each of Cd(II) and Pb(II) on an in situ plated BiF/NA/GCE (dotted line), BiF/SWNTs–NA/GCE (dashed line), and BiF/GNFs–NA/GCE (solid line). Supporting electrolyte 0.10 M acetate buffer (pH 4.5), deposition potential −1.2 V, deposition time 120 s, quiet time 10 s, amplitude 80 mV, increment potential 5 mV, pulse period of 0.2 s, and pulse width of 5 ms.

The effect of the deposition potentials on metal stripping signals were studied with 20 μg L^{-1} each of Cd(II) and Pb(II) with deposition time of 120 s in the range from −0.9 up to −1.4 V. When the deposition potential shifts from −0.9 to −1.2 V, the stripping peak currents increase sharply, as displayed in Fig. 4(B). As the deposition potential becoming more negative, the reproducibility of stripping currents of Cd and Pb becomes poor, because hydrogen evolution is beginning to be significant in acetate buffer at such negative potential [28]. The metal alloys deposited on the electrode surface might be damaged by the hydrogen bubble and lead to decrease in current signals at very negative potentials. Therefore, −1.2 V was selected for the following experiments due to good sensitivity.

The effect of the deposition time on the stripping peak currents was also studied from 30 s up to 600 s. As can be seen from Fig. 4(C), as the accumulation time increased from 30 s to 120 s, the stripping peak currents of Cd(II) and Pb(II) increased linearly. However, the linear trend was not obvious with the further prolonging of the deposition time, only a slight increase of the stripping responses was found due to the saturation loading on the electrode surface. Thus, an accumulation time of 120 s was chosen as the optimal accumulation time.

As shown in Fig. 4(D), the influence of the concentrations of Bi(III) was studied in the range from 100 to 1000 μg L^{-1}, each containing 20 μg L^{-1} of Cd(II) and Pb(II) with deposition time of 120 s. The heights of the stripping peaks displayed a clear dependence on the Bi film thickness as they increased with increasing concentrations of bismuth ions from 100 to 400 μg L^{-1}. However, for

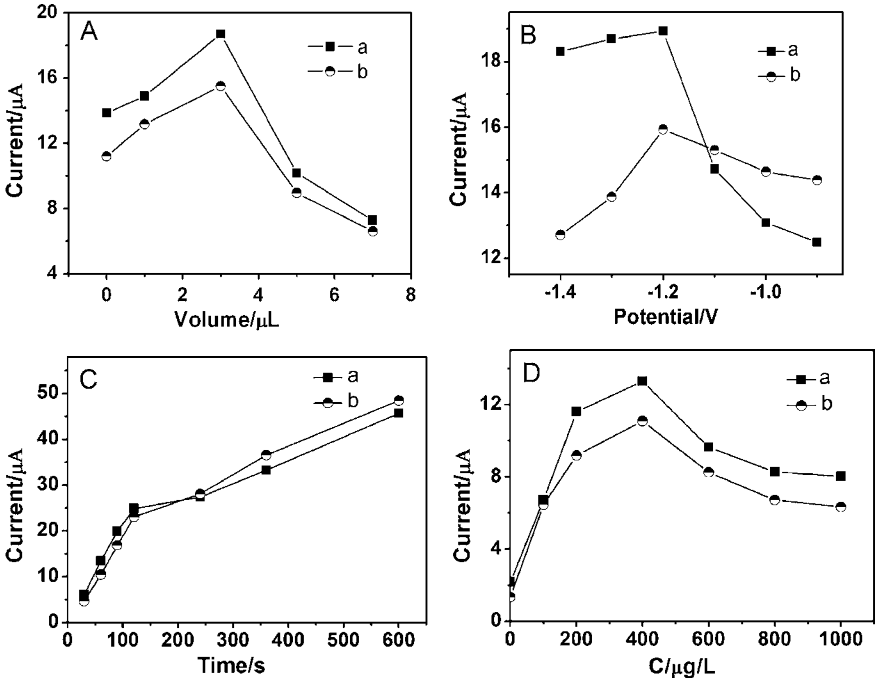

Fig. 4. Effect of the volume of GNFs–NA suspension (A), deposition potential (B), deposition time (C), and concentration of Bi(III) (D) on the stripping peak current of 20 μg L^{-1} each of Cd(II) (a) and Pb(II) (b) on the in situ plated BiF/GNFs–NA/GCE. Other conditions as in Fig. 3.

Bi(III) concentrations higher than 400 μg L^{-1}, the stripping peak currents of Cd(II) and Pb(II) decreased gradually and both of the peaks became wider, which is probably due to the fact that thick bismuth film may hinder the mass transfer of metal ions during the stripping step [29]. Therefore, the optimized concentration of bismuth was chosen as 400 μg L^{-1}.

3.4. Calibration data

Calibration plots for the simultaneous determination of Cd(II) and Pb(II) on the BiF/GNFs–NA/GCE were achieved by DPASV under the optimal conditions. The DPASV for different concentrations of Cd(II) and Pb(II) were illustrated in Fig. 5. The resulting calibration plots are linear over the range from 0.2 to 50 μg L^{-1} for both Cd(II) and Pb(II). The calibration curves and correlation coefficients are $y = -0.03114 + 0.9780x$, $r = 0.9969$ and $y = -0.9012 + 1.3174x$, $r = 0.9995$ for Cd(II) and Pb(II) with a preconcentration time of 120 s, respectively (x: concentration/μg L^{-1}, y: current/μA). The limits of detection were 0.26 μg L^{-1} for Cd(II) and 0.19 μg L^{-1} for Pb(II) based on three times the background noise. Longer deposition time led to higher sensitivity. Under the same conditions, the limits of detection were 0.09 μg L^{-1} for Cd(II) and 0.02 μg L^{-1} for Pb(II) with a preconcentration time of 10 min, which are more sensitive than those of NA modified BiFEs (0.1 μg L^{-1} for Cd(II) and Pb(II) [23]) and OMC-NA coated GCE (0.95 μg L^{-1} for Pb(II) [14]). When compared with the CNTs–NA coated BiFE [13] and graphene–NA coated BiFE [16], the present method exhibited the comparable sensitivity. The reproducibility of BiF/GNFs–NA/GCE was evaluated by 16 repetitive measurements of Cd(II) and Pb(II). The relative standard deviations were 1.4% and 2.1% for 20 μg L^{-1} each of Cd(II) and Pb(II), respectively. The results demonstrated that the modified electrode could improve both the sensitivity and the reproducibility of bismuth-modified electrode.

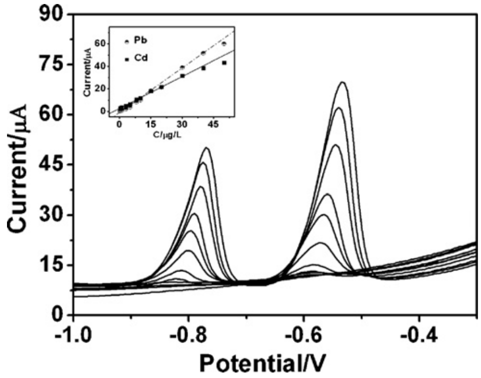

Fig. 5. Stripping voltammograms for the different concentrations of Cd(II) and Pb(II) on an in situ plated BiF/GNFs–NA/GCE in solution containing 400 μg L^{-1} Bi(III). From bottom to top, 0.2, 0.6, 1.0, 3.0, 5.0, 10, 15, 20, 30, 40, and 50 μg L^{-1} Cd(II) and Pb(II), respectively. (Inset) the calibration curves of Cd(II) and Pb(II), respectively. Other conditions as in Fig. 3.

3.5. Interferences

The common existing interferences of inorganic species were investigated to test the selectivity, as well as the influence of some other surface-active compounds. It was found that 1000-fold for K^+, Mg^{2+}, Ca^{2+}, SCN^-, Br^-, NO_3^-, PO_4^{3-}, and SO_4^{2-}, have no influences on the signal of 20 μg L^{-1} of Cd(II) and Pb(II). The tolerated ratio of the other substances was 200-fold for Fe^{3+}, 100-fold for Zn^{2+}, 50-fold for MnO_4^-. Triton X-100, cetyltrimethylammonium bromide (CTAB), and sodium dodecyl sulfate (SDS) were selected as the model compound to study the possible interferences with the stripping voltammetric measurements of heavy metal ions at the BiF/GNFs–NA/GCE and BiF/NA/GCE. The peak currents of metal ions before (I_{pmax}) and after adding different surfactants (I_p) were recorded. Table 1 shows the data on the normalized current, I_p/I_{pmax}, at different surfactants for both electrodes. Compared with the BiF/NA/GCE, the BiF/GNFs–NA/GCE presented better antifouling ability to surfactants, which may be attributed to the different interfacial properties of the bismuth film electrode [22]. This implies the possible direct application of BiF/GNFs–NA/GCE in real samples which contain low concentration of surfactants.

Table 1
Normalized current, I_p/I_{pmax}, expressed as a percentage, for 20 μg L^{-1} each of Cd(II) and Pb(II) at 5 mg L^{-1} surfactants for the BiF/NA/GCE and BiF/GNFs–NA/GCE, respectively.

Metal ion	Electrode	(I_p/I_{pmax}/%)		
		Triton X-100	CTAB	SDS
Cd(II)	BiF/NA/GCE	53	36	70
	BiF/GNFs–NA/GCE	57	83	107
Pb(II)	BiF/NA/GCE	38	55	89
	BiF/GNFs–NA/GCE	49	96	102

3.6. Application

The as-prepared electrode was used to determination of Cd(II) and Pb(II) in real samples. Standard additions of 2 μg L^{-1} each of Cd(II) and Pb(II) caused current increments at the sample potentials and made the determination of Cd(II) and Pb(II) in the river water possible. The values of Cd(II) and Pb(II) in river water were calculated to be 0.75 ± 0.05 and 2.33 ± 0.05 μg L^{-1}, which are consistent with the results obtained by ICP-MS (0.70 ± 0.04 for Cd(II) and 2.50 ± 0.04 μg L^{-1} for Pb(II), respectively). For the human blood sample, standard additions of 5 μg L^{-1} Pb(II) each to the sample with a preconcentration time of 120 s, we got 66.25 ± 0.88 μg L^{-1} of Pb(II) in the blood sample (Cd(II) is not found), which is consistent with the results obtained by ICP-MS (63.13 ± 1.37 μg L^{-1}). From these results, we can conclude that the as-prepared electrode could provide a satisfactory method for the determination of metal ions in real samples.

4. Conclusion

GNFs, as a promising carbon material, was used to fabricate modified electrode for the simultaneous determination of Cd(II) and Pb(II). The as-prepared electrode has the advantages of high electrical conductivity and high resistance to organic interferences compared with bare GCE. In addition, the as-prepared electrode was successfully applied to the real samples and the results agree well with those of ICP-MS.

Acknowledgments

This project was supported by the National Basic Research Program of China (2010CB933603), the State Plan for High-Tech Research and Development (2007AA061501), the National Natural Science Foundation of China (nos. 20820102037 and 20805044), and the Foundation of Young Scholars of Jilin Province (20080123).

References

[1] J. Wang, Stripping Analysis: Principles, Instrumentation and Applications, VCH, Deerfield Beach, FL, 1985.
[2] J. Wang, Analytical Electrochemistry, 3rd ed., Wiley, Hoboken, New Jersey, 2006.
[3] J. Wang, Electroanalysis 17 (2005) 1341–1346.
[4] A. Economou, TRAC—Trends Anal. Chem. 24 (2005) 334–340.
[5] A. Economou, P.R. Fielden, Analyst 128 (2003) 205–212.
[6] J. Wang, J.M. Lu, S.B. Hocevar, P.A.M. Farias, B. Ogorevc, Anal. Chem. 72 (2000) 3218–3222.
[7] S. Legeai, O. Vittori, Anal. Chim. Acta 560 (2006) 184–190.
[8] L. Baldrianova, I. Svancara, M. Vlcek, A. Economou, S. Sotiropoulos, Electrochim. Acta 52 (2006) 481–490.
[9] S. Legeai, S. Bois, O. Vittori, J. Electroanal. Chem. 591 (2006) 93–98.
[10] J. Wang, J.M. Lu, U.A. Kirgoz, S.B. Hocevar, B. Ogorevc, Anal. Chim. Acta 434 (2001) 29–34.
[11] W. Yantasee, L.A. Deibler, G.E. Fryxell, C. Timchalk, Y.H. Lin, Electrochem. Commun. 7 (2005) 1170–1176.
[12] D. Sun, X.F. Xie, Y.P. Cai, H.J. Zhang, K.B. Wu, Anal. Chim. Acta 581 (2007) 27–31.
[13] H. Xu, L.P. Zeng, S.J. Xing, Y.Z. Xian, G.Y. Shi, Electroanalysis 20 (2008) 2655–2662.
[14] L.D. Zhu, C.Y. Tian, R.L. Yang, J.L. Zhai, Electroanalysis 20 (2008) 527–533.
[15] P. Sonthalia, E. McGaw, Y. Show, G.M. Swain, Anal. Chim. Acta 522 (2004) 35–44.
[16] J. Li, S.J. Guo, Y.M. Zhai, E.K. Wang, Anal. Chim. Acta 649 (2009) 196–201.
[17] J. Li, S.J. Guo, Y.M. Zhai, E.K. Wang, Electrochem. Commun. 11 (2009) 1085–1088.
[18] V. Vamvakaki, K. Tsagaraki, N. Chaniotakis, Anal. Chem. 78 (2006) 5538–5542.
[19] L. Li, C.M. Lukehart, Chem. Mater. 18 (2006) 94–99.
[20] P. Werner, R. Verdejo, F. Wollecke, V. Altstadt, J.K.W. Sandler, M.S.P. Shaffer, Adv. Mater. 17 (2005) 2864–2869.
[21] S.U. Kim, K.H. Lee, Chem. Phys. Lett. 400 (2004) 253–257.
[22] J. Wang, R.P. Deo, S. Thongngamdee, B. Ogorevc, Electroanalysis 13 (2001) 1153–1156.
[23] G. Kefala, A. Economou, A. Voulgaropoulos, Analyst 129 (2004) 1082–1090.
[24] C.Y. Yang, J.X. Huo, X.Y. Zhang, Stud. Trace Elem. Health 21 (2004) 49–50.
[25] L.N. Wu, X.J. Zhang, H.X. Ju, Anal. Chem. 79 (2007) 453–458.
[26] P. Chen, R.L. McCreery, Anal. Chem. 68 (1996) 3958–3965.
[27] H.J. Chen, Y.L. Wang, Y. Liu, Y.Z. Wang, L. Qi, S.J. Dong, Electrochem. Commun. 9 (2007) 469–474.
[28] R. Pauliukaite, C.M.A. Brett, Electroanalysis 17 (2005) 1354–1359.
[29] L.Y. Cao, J.B. Jia, Z.H. Wang, Electrochim. Acta 53 (2008) 2177–2182.